
Design study

NSF#1 Pile HKZ

Document information

Date	: 16 January 2024
Company	: Aqitec
Client	: North Sea Farmers
Version	: 1.0
Document status	: For permit application
Classification	: Report
Nr of pages	: 29
Written by	: I.W. Wieling, I.S. Wieling
Project approval	:
Detailed approval	:
Basic approval	:

Contents

1. Version control.....	3
2. Introduction	4
2.1. References.....	4
3. Input and requirements	5
3.1. Input	5
3.2. Global scour.....	6
3.1. Material	7
4. Approach.....	8
4.1. General approach	8
4.2. Lateral soil resistance	8
4.3. Axial soil resistance.....	8
4.4. Pile structural check.....	9
4.5. Axial/lateral utilization	9
4.6. Pad-eye strength	10
5. Concept design.....	11
6. Structural report.....	12
6.1. ULS - Axial soil resistance	12
6.2. ULS - Lateral soil resistance.....	13
6.3. ULS - Pile structural check	16
6.4. ALS load case.....	18
6.5. Pad-eye	18
6.6. Fatigue.....	23
7. Conclusion.....	24
Appendix A: Anchor loads from simulation results	25
Appendix B: Fit shackle.....	28

1. Version control

Document version nr.	Date	Changes	Remarks
1.0	16-01-2024	For permit application	

1.1.1. Disclaimer

Do not copy, cite or distribute without prior permission of the author.

2. Introduction

The consortium led by North Sea Farmers will develop the North Sea Farm #1 (NSF#1) with Aqitec providing consultancy on the design. This seaweed farm will be integrated into the Hollandse Kust Zuid wind farm.

The seaweed farm is anchored by two piles on either side of the system.

A report by BT Geoconsult BV is available providing recommended locations for the anchoring pile and the corresponding soil properties [9].

2.1. References

- [1] Aqitec; 20230302_NSF1_structural_v1.1; 2 March 2023
- [2] Van Oord Offshore; 144978-VOOW-TF-ENG-TN-1001 Anchor piles - Soil parameters assessment and geotechnical design recommendations; 01 September 2023
- [3] Aqitec; 20230707_NSF1_design_basis_v2.1; 7 July 2023
- [4] Aqitec; 20230330_Recommended_design_practice_v1.0; 30 March 2023
- [5] API RP 2GEO, Geotechnical and Foundation Design Considerations, 2011
- [6] NS9415:2021, Floating aquaculture farms, Site survey, design, execution and use
- [7] Taiebat, Hossein & Carter, John. (2005). A Failure Surface for Caisson Foundations in Undrained Soils. 289-296. 10.1201/NOE0415390637.ch25.
- [8] Deltares, Morphodynamics of Hollandse Kust (zuid) Wind Farm Zone, 1230851-000-HYE-0003, Final, 22 December 2016
- [9] BT Geoconsult BV; Soil interpretation anchor piles; **Draft; 18 October 2023**
- [10] Van der Straaten, offerte, 71129-OFF-0.2-001-EDE

3. Input and requirements

3.1. Input

Table 1: Soil design properties [9].

				Submerged soil unit weight	Internal friction angle (low estimate)	Internal friction angle (high estimate)	Skin friction angle (low estimate)	Skin friction angle (high estimate)	Initial modulus of subgrade reaction
Layer	Depth from	Depth to	Description	γ'	LE ϕ'	HE ϕ'	LE δ	HE δ	k
[-]	[m]	[m]	[-]	[kN/m ³]	[°]	[°]	[°]	[°]	[kN/m ³]
A	0	0.5	Sand, loose to medium dense	9	30	40	20	25	11 000
B	0.5	1	Sand, medium to very dense	10	39	45	25	35	40 000
C	1	16	Sand, dense to very dense	10	42	46	30	35	45 000
D	16	30	Sand, medium to dense	10	37	43	25	30	31 000

3.1.1. General requirements

Design life	10 year	[3]
Local scour	1.5 x D	[2]
Global scour	1.0m	[see next section]
Decommissioning by vibratory hammer after 10y.		[3]

3.2. Global scour

An estimate for global scour is extracted from [8]. This report by Deltares shows the maximum predicted seabed lowering between 2016 and 2051. The image below visualizes the Deltares results overlain by the recommended locations from the soil interpretation report [9].

The selected areas show an average maximum predicted seabed lowering between 0.5m – 1.0m. Therefore a global scour of 1.0m is assumed.

Maximum predicted seabed lowering is larger when selecting the top of the sand dune or just in front of the top of the sand dune based on sand travel direction; during placement of the pile these areas must be avoided. According to [8] the typical migration speed of sand waves in site II and IV is 1.5-1.7 meter per year in 28° North direction. 90% non-exceedance migration speed range up to 3.0 meter per year. For the 10 year design life it is expected that sand waves typically move 15m in NNE-NE direction up to 30 meter with 90% exceedance. **It is advised to install the anchor piles at least 60 meter NNE of the trough (Nederlands=dal) and (up to) 60m SSW of the crest (Nederlands=top) of sand waves.**

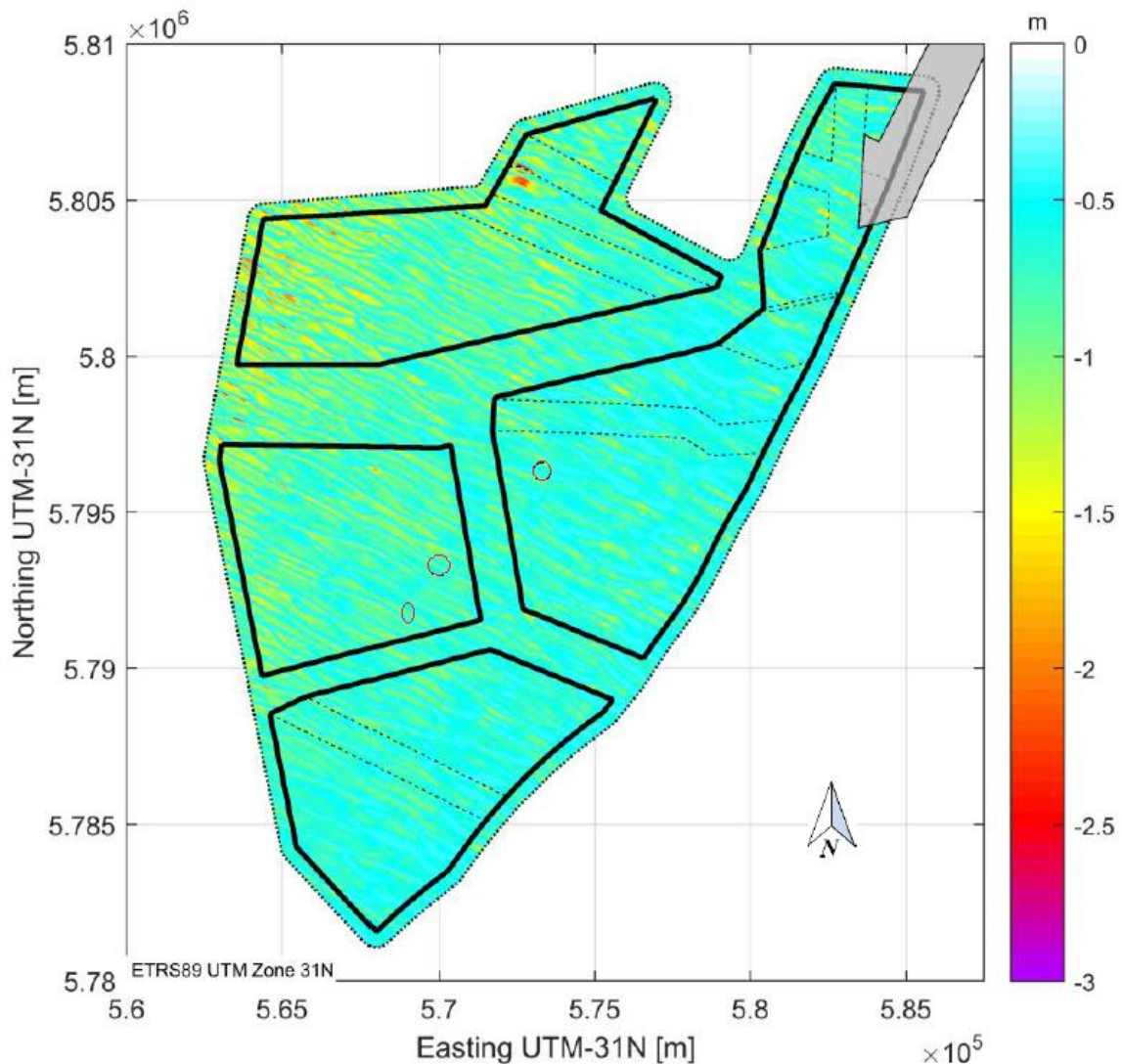


Figure 1: The maximum predicted seabed lowering including the downward uncertainty band based on the 2016 Bathymetry. Values indicate the difference between the 2016 Bathymetry and the LSBL from [8] overlain with the recommended locations (3 circles) from [9].

3.2.1. Load cases and pile stability requirements

Table 2: Load cases and safety, material and load factors

Load case		General		Soil resistance (geotechnical)	Pile capacities (structural)	
		Max. load** [Appendix A]	Horizontal out-of-plane angle***	Safety factor [2]	Load factor [4]	Material factor [4]
		[kN]	[°]	[-]	[-]	[-]
ULS #1*	Lateral (horizontal)	688.8	21.6 (±2.5)	1,60	1,15	3
	Axial (vertical)	212.5		2,00		
ULS #2*	Lateral (horizontal)	653.0	23.4 (±2.5)	1,60	1,15	3
	Axial (vertical)	268.0		2,00		
ALS*	Lateral (horizontal)	337.9	Not applicable	1,20	1,0	2
	Axial (vertical)	47.9		1,50		

*Load cases are extracted from Appendix A. ULS#1 is extracted from the load case with the highest lateral anchor load (LC#17) and ULS#2 is extracted from the load case with the highest axial anchor load (LC#24). ALS is extracted from the load case with the highest lateral and axial anchor load (LC#209).

Appendix A gives the anchor forces and angles at the moment of highest lateral and axial force in each load case. As a conservative approach the maximum lateral and axial anchor loads during the simulations are assumed to apply simultaneously. The horizontal out-of-plane angle is taken when the maximum lateral (ULS#1) and maximum axial (ULS#2) anchor loads apply. The horizontal out-of-plane angle is not applicable due to the geometry of the load case, more detail on this later in this report.

** The given loads apply at the seabed level.

*** The horizontal angle between the anchor load and the imaginative line between the two anchors is meant with horizontal out-of-plane angle. Installation tolerance within brackets [2]

A maximum pile deflection of 10% of the pile outer diameter at the seabed level is generally accepted as criterion for pile stability i.e. to determine the pile embedment length. [2]

It is recommended to have a pile embedment depth which avoids a pile 'toe kick'. This is achieved when the pile deflection at the seabed is not influenced by further pile length increase. [2]

3.2.2. Requirements corrosion

Source corrosion requirements [2]. Corrosion:

- Submerged zone: everything above seabed (inside & outside): 0.10 [mm/yr/side]
- Upper sediment zone: until 5 [m] below seabed (inside & outside): 0.10 [mm/year/side] + 0.10 [mm/yr/side] due to MIC (Microbiologically Induced Corrosion)
- Buried zone: 5 [m] below seabed and below that: 0.0 [mm/yr/side]

Design life of 10 year:

- Submerged zone: 2mm reduction wall thickness
- Upper sediment zone: 4mm reduction wall thickness

3.1. Material

L485ME (pipe body) according [10].

Yield strength Rp0,5 min. 485 Mpa

Tensile strength Rm min. 570 Mpa

S355 (pad-eye)

Tensile strength Rm min. 470 Mpa

4. Approach

4.1. General approach

The chain is at/above the seabed and calculated hydrodynamic loads are considered to act directly on the pad-eye.

The load cases take into account minimum and maximum scouring, lower and higher estimate of soil parameters.

The axial capacities are evaluated. Based on the axial utilization ratio, the maximum allowed lateral utilization ratio (based on [7]) and minimum required lateral capacities are verified.

The overall dimensions are determined by five main criteria:

- Ø1220x21 and Ø1220x21.9 Piles - material L485ME - are sourced
- Axial capacity
- 'Toe kick' requirement
- Maximum allowed stress
- Maximum 10% pile deflection at seabed level

Based on the above criteria a pile with penetration depth of 11 meter and 2 meter stick-out is selected. The pad-eye is located on the seabed. The pile toe-kick was found to be the critical requirement for pile length. Lower pad eye positions have been evaluated, but proved to have just a small effect on the toe-kick. In other words, lowering the pad-eye 1 to 3 meter below the seabed results in 0.5 to 1.5m less penetration depth. The benefits of having the pad-eye above the seabed is considered to be advantageous for following reasons:

- Inspection of the chain, shackle and pad eye position
- Strength of the soil will result in minimal inverted catenary of the chain and ineffective use of the pile lateral capacity
- The pad-eye, shackle and chain do not need to be embedded during vibratory hammering
- With a pad-eye below the seabed repeated axial loads (due to chain-soil interaction) can theoretically lead to premature failure.
- Simpler pad-eye design

No alternative pile diameters have been investigated as the given pipe is sourced prior to this study.

Practical aspects need to be evaluated, but are considered out-of-scope for this study:

- Manufacturability
- Size, weight, handling on-board
- Drivability with vibratory hammer
- Retrieval

4.2. Lateral soil resistance

Software package PyPile is used to examine the lateral soil resistance. Soil is modelled according API guidelines [5]. Lateral soil resistance is calculated by applying the minimal resistance (=max load * safety factor/utilization ratio) to the model while using the load-case specific friction angle estimates for the soil. Cyclic loading is taken into account in the P-y curve. Global scouring is applied by removing the layer fully, local scouring is applied by removing the load bearing capacity of the layer, however submerged unit weight is retained to reflect the overburden pressure in deeper layers.

The pile is modelled with 200 bins over the length of the pile. The analysis is done with the nominal wall thickness.

4.3. Axial soil resistance

Axial soil capacity is calculated according the guidelines in [5] (similar to DNV-OS-J101). The following formula is used:

$$f_s = K p_0' \tan \delta \leq f_l$$

with

f_s	Average unit skin friction	
K	Coefficient of lateral earth pressure	(For open ended piles $K=0.8$)
p_0'	Overburden pressure	(Calculated with submerged soil unit weight from Table 1)
δ	Skin friction	(from Table 1)
f_l	Limiting unit skin friction	(According DNV-OS-J101)

A dedicated sheet is prepared that calculates the axial capacity based on the formula above. Note that the capacity is determined based on an upward load, thus end bearing capacity is not considered. Calculation of overburden pressure (p_0') is performed by assuming soil removed from global scour does not contribute, however the soil layer removed by local scour does contribute to the overburden pressure. The sheet selects the minimum value between the plugged and unplugged state as follows:

Unplugged: Axial Capacity = Pile submerged weight + External skin friction + Internal skin friction

Plugged: Axial Capacity = Pile submerged weight + Plug submerged weight + External skin friction

Pile capacities are determined for each combination of soil properties (High / Low Estimate) and the inclusion/exclusion of (local and global) scour. Interaction of the pad-eye with the soil is expected to increase the axial capacity slightly, however is neglected in the determination of the axial capacity. Results of this analysis can be found in Table 5.

4.4. Pile structural check

Von Mises stress in the pile is calculated based on the results from PyPile for shear and moment across the length of the pile combined with the stress from the axial load (maximum axial load is conservatively assumed to act throughout the pile). The normal stress from PyPile and the axial load are added together before calculating the Von Mises stress.

Lateral shear and moment are calculated by applying the respective load (=max load * load factor / utilization ratio) to the model while using the load-case specific friction angles and applicable inclusion/exclusion of scouring.

No stress concentration factors are applied during this structural check. Corrosion is included for the top 5 meter below the seabed. A detailed analysis of the pad-eye follows later in the report that accounts for the (at this moment neglected) stress concentration factors.

A buckling check is performed according DNV-RP-C202 Sec 3.2-Sec 3.4.

The effect of including/excluding cyclic loading is checked as a final step.

4.5. Axial/lateral utilization

Lateral and axial soil resistance are evaluated separately for simplicity. However according [2] a load angle above 15 degrees could induce load coupling; vertical load angles above 15 degrees are found in the simulation results (see Appendix A).

Van Oord Offshore advised to use utilization ratios for suction caissons taken from [7]. According Van Oord Offshore this is thought to be conservative for pile design, as the effect of an interaction between axial and lateral load on a suction caisson should be greater.

The applicability of the paper [7] is reasonable, however piles and suction caissons have a very different D/L. Furthermore the paper seems to use cohesive soils (clay), whereas all calculations performed on the pile assume cohesionless soil. Their method of calculating ultimate axial/lateral resistance is therefore also different compared to the method used in this report.

The solid brown line in Figure 2 is selected to determine the axial/lateral utilization ratio. The pile has nominal $z/L = 0.0$ and $D/L > 10$. Decrease in utilization ratio caused by scouring ($z/L \sim 0.25$) is assumed to be offset by the larger D/L .

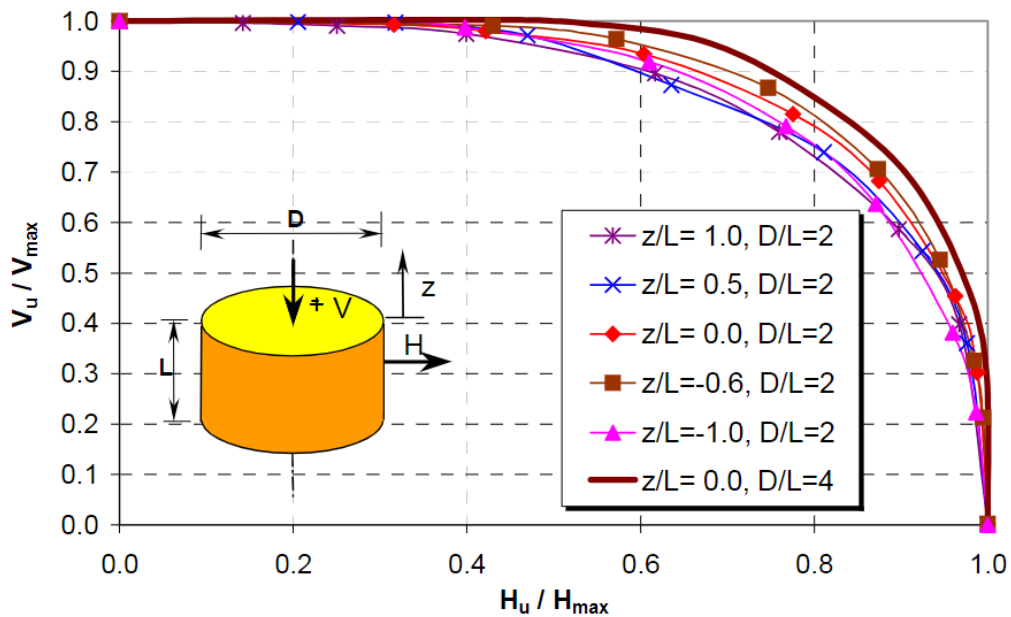


Figure 2: Non-dimensional failure locus in the axial-lateral loading plane, taken from [7]

4.6. Pad-eye strength

Pad-eye strength is calculated by applying the load cases with maximum horizontal and vertical loads calculated from the chain-soil interaction to the pad-eye in FEM, material factors are added to evaluate the results. Hand calculations are used to verify the FEM results.

A linear FEM is performed, assuming all stresses are below the yield point of the material.

5. Concept design

Table 3: Concept design main particulars

Pile weight	[kg]	8339
Pile length	[m]	13
Pile diameter	[mm] [inch]	1219 48
Pile wall thickness	[mm]	21 / 21.9
Eco-structure height/ stick-out	[m]	2.0
Pad-eye height (measured from nominal seabed)	[m]	0.125
Eye diameter*	[mm]	112
Material pile	[-]	L485ME
Material pad eye	[-]	S355J2G3 or S355NL0**

*Oval pin LTM anchor shackle type D has section 1.9xD and 1.1xD. Chain diameter is $\varnothing 58$. Hole diameter pad-eye $\varnothing 110.2\text{mm}$
 ** Material in consultation with production company. From structural point S355 is required

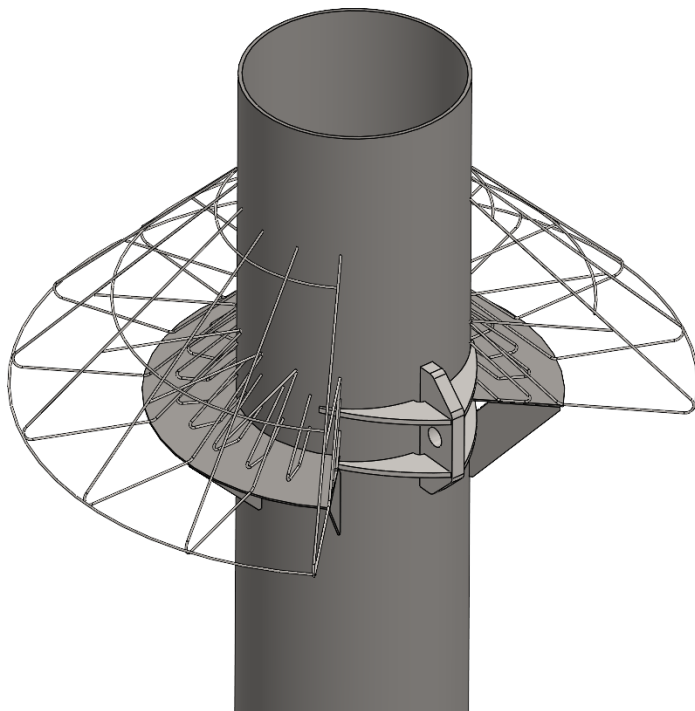


Figure 3: Concept design eco structure

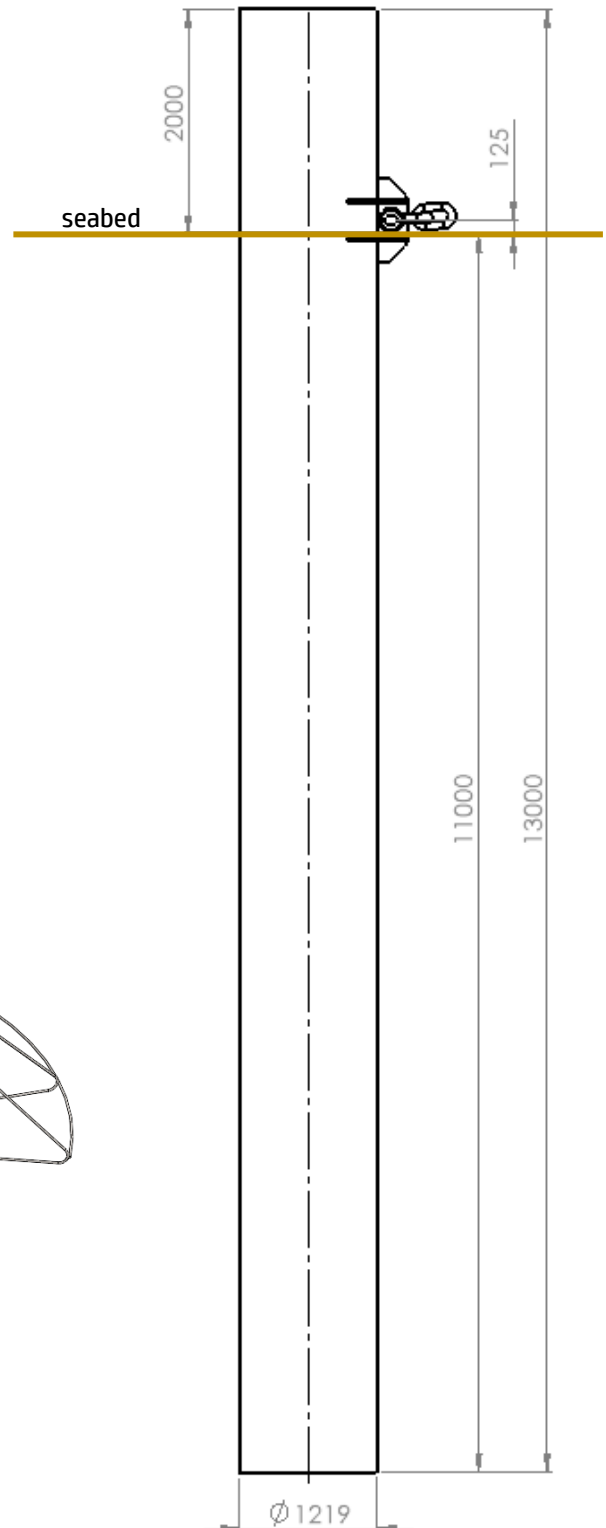


Figure 4: Concept design without eco structure

6. Structural report

6.1. ULS - Axial soil resistance

Calculation of the axial soil resistance for each of the load cases stated in Table 5 shows required and calculated axial capacity of the pile and all axial load cases are within limits. Included in the axial capacity is 47 kN submerged pile weight and 120 kN submerged plug weight. PLC#...A are based on ULS#1 and PLC#...B are based on ULS#2.

An axial utilization ratio (V/V_u) is calculated and a minimum lateral utilization ratio (H/H_u) is determined based on [7]. With the minimum lateral utilization ratio a set of minimum required lateral resistances is calculated, which are further analyzed in the next section of this report.

Table 4: Input for determining the axial soil resistance.

Global scouring <i>Sand fully removed</i>	1m
Local scouring <i>Sand contributes to overburden pressure of layers below</i>	$1.5 \cdot 1.219 = 1.83\text{m}$
Scouring, total	2.83m
Direction	Tension

Table 5: Axial capacity vs minimum resistance. Horizontal utilization ratio and subsequent vertical utilization ratio and required lateral resistance.

ULS pile load case	Skin friction Angle		Axial Capacity ¹ [kN]	Required Axial Capacity ² [kN]	Vertical utilization ratio ³ [V/V _u]	Required Lateral Soil Resistance without utilization ratio ⁴ [kN]	Maximum horizontal utilization ratio ⁵ [H/H _u]	Required lateral soil resistance with utilization ratio ⁶ [kN]	Lateral structural load ⁷ [kN]	Axial structural load ⁷ [kN]
PLC#1A	LE	Excluding scouring	1231	425	0.35	1102	0.99	1113	792	244
PLC#1B				536	0.44	1045	0.98	1066	751	308
PLC#2A	HE		1459	425	0.29	1102	1.00	1102	792	244
PLC#2B				536	0.37	1045	0.99	1055	751	308
PLC#3A	LE	Including scouring	1023	425	0.42	1102	0.98	1125	792	244
PLC#3B				536	0.52	1045	0.96	1088	751	308
PLC#4A	HE		1204	425	0.35	1102	0.99	1113	792	244
PLC#4B				536	0.45	1045	0.98	1066	751	308

¹) Calculation of axial capacity of soil according DNV-OS-J101

²) From ULS#1 and ULS#2 including safety factor (2)

³) Required Axial Capacity / Axial Capacity

⁴) From ULS#1 and ULS#2 including safety factor (1.6)

⁵) According failure envelope from [7] based on vertical utilization ratio

⁶) Required capacity including safety factor (1.6) and horizontal utilization ratio

⁷) Required capacity including load factor (1.15)

6.2. ULS - Lateral soil resistance

The minimum required ultimate lateral resistance as given in Table 5 is evaluated in this section to confirm the design is within the utilization envelope.

Model parameters:

- Global scouring 1.0m
 - o When scour included: Fully removed
- Local scouring $1.5 \times D = 1.5 \times 1.219 = 1.83\text{m}$
 - o When scour included: No lateral capacity; effective soil weight to calculate overburden pressure on layers below
- API sand
- Cyclic loading
- E-modulus steel 210 GPa
- Density of steel 7800 [kg/m³]



Figure 5: Pile model in PyPile, with and without scour. With scour the stick out (global scour) is 1.0m.

Table 6: Soil properties used as input in PyPile – no scouring

Layer	Depth from [m]	Depth to [m]	γ' [kN/m ³]	LE ϕ' [°]	HE ϕ' [°]	k [kN/m ³]
A	0	0.5	9	30	40	11.000
B	0.5	1	10	39	45	40.000
C	1	16	10	42	46	45.000

Table 7: Soil properties used as input in PyPile – with scouring

Layer	Depth from [m]	Depth to [m]	γ' [kN/m ³]	LE ϕ' [°]	HE ϕ' [°]	k [kN/m ³]
Stick-out	-1.0					
Scouring	0	1.83	9	0	0	0
C	1.83	16	10	42	46	45.000

Table 8 presents the deflection at seabed for ULS pile load cases including utilization factor according Table 5. For all cases the deflection at seabed level is below the 10% x OD (122mm) deflection criterion.

The pile satisfies the ‘toe kick’ requirement for the 11.0m length pile; the deflection remains constant for increased pile lengths. The deflection at the seabed is visually shown in Figure 6 for PLC#3 the deflection of a 11.0m pile at seabed is 0.4mm higher compared to longer piles. 0.4mm is accepted to be within the limits to consider this constant.

Table 8: Deflection at seabed [mm] for the ULS pile load cases. Pile includes corrosion. Lateral load without utilization factor (1102kN)

Pile Length [m]			8	8.5	9	9.5	10	10.5	11	11.5	12	12.5
Load case												
PLC#1	Skin friction angle LE	Excluding scouring	32	28	27	26	26	26	26	26	26	26
PLC#2	Skin friction angle HE	Excluding scouring	23	22	21	21	21	21	21	21	21	21
PLC#3	Skin friction angle LE	Including scouring	143	71	50	43	40	39	38	38	38	38
PLC#4	Skin friction angle HE	Including scouring	60	43	38	35	34	33	33	33	33	33

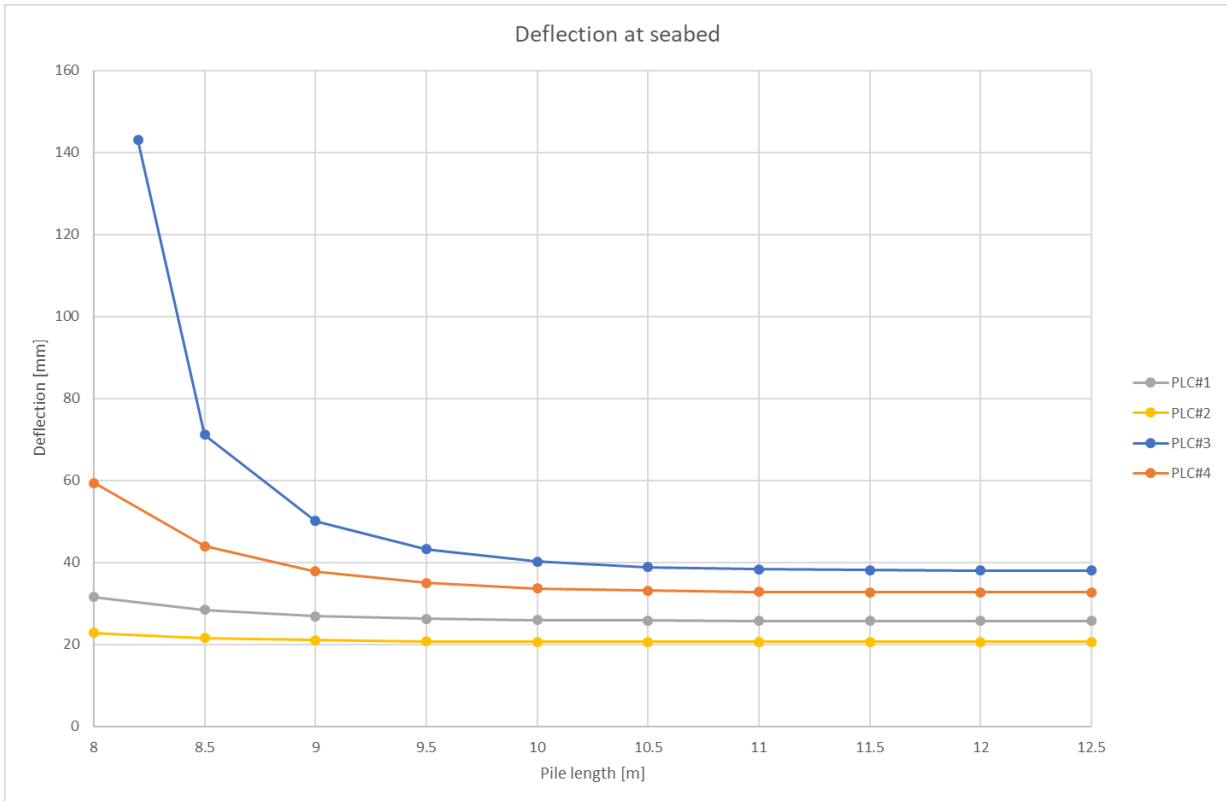


Figure 6: Deflection at seabed for load cases (From Table 8)

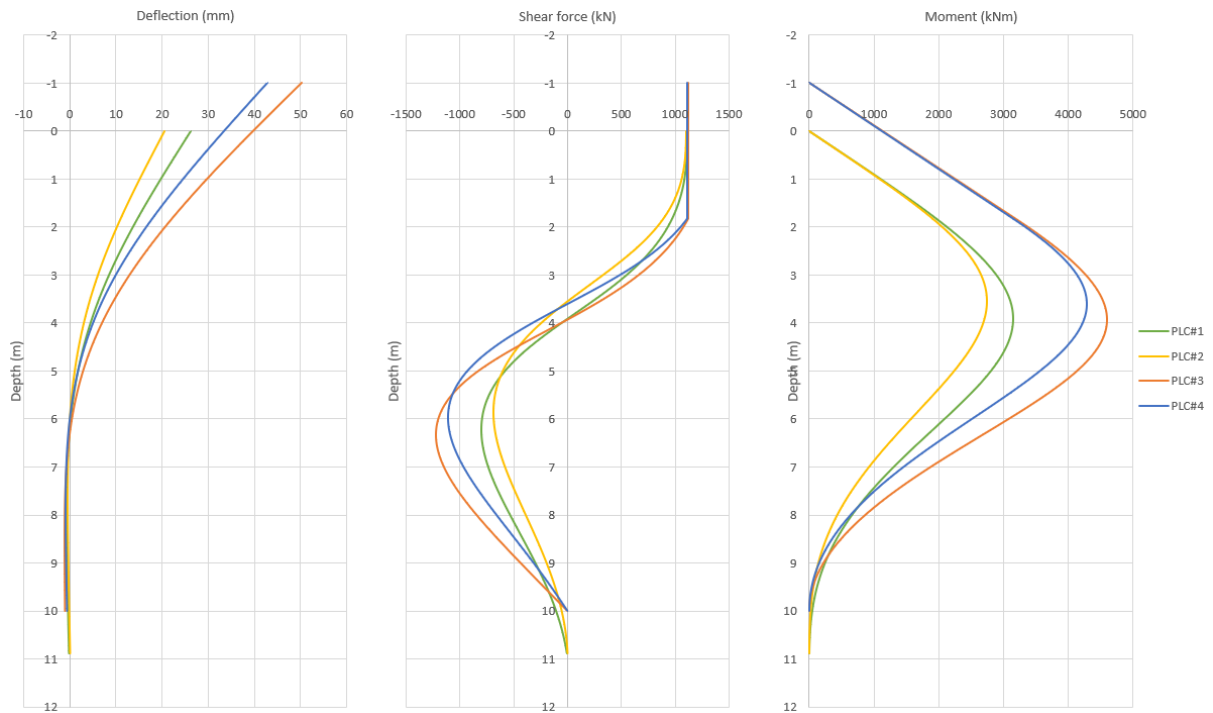


Figure 7: Deflection, shear force and moment for PLC#1-PLC#4. Zero depth is the seabed location for PLC#3 and PLC#4 includes global scouring (-1.0m).

6.3. ULS - Pile structural check

Load cases for the structural check are shown in Table 5. As a conservative approach load cases PLC#...A and PLC#...B are combined by taking the maximum lateral and axial load amongst the load cases and combining them as given in Table 9.

Table 9: ULS load cases at pad-eye for structural check

ULS pile load case	Skin friction Angle		Axial load [including load factor] [kN]	Lateral load [including load factor] [kN]
PLC#1	LE	Excluding scouring	792	308
PLC#2	HE		792	308
PLC#3	LE	Including scouring	792	308
PLC#4	HE		792	308

Cyclic loading is taken into account in the lateral load analysis. Results can be seen in Figure 8. Excluding cyclic loading decreases stresses. The pile satisfies the requirement for pile capacity; the maximum stress found for PLC#3 of 164MPa is below the maximum allowed stress level for ULS after taking into account the material factor: $R_m/3=570/3=190\text{MPa}$.

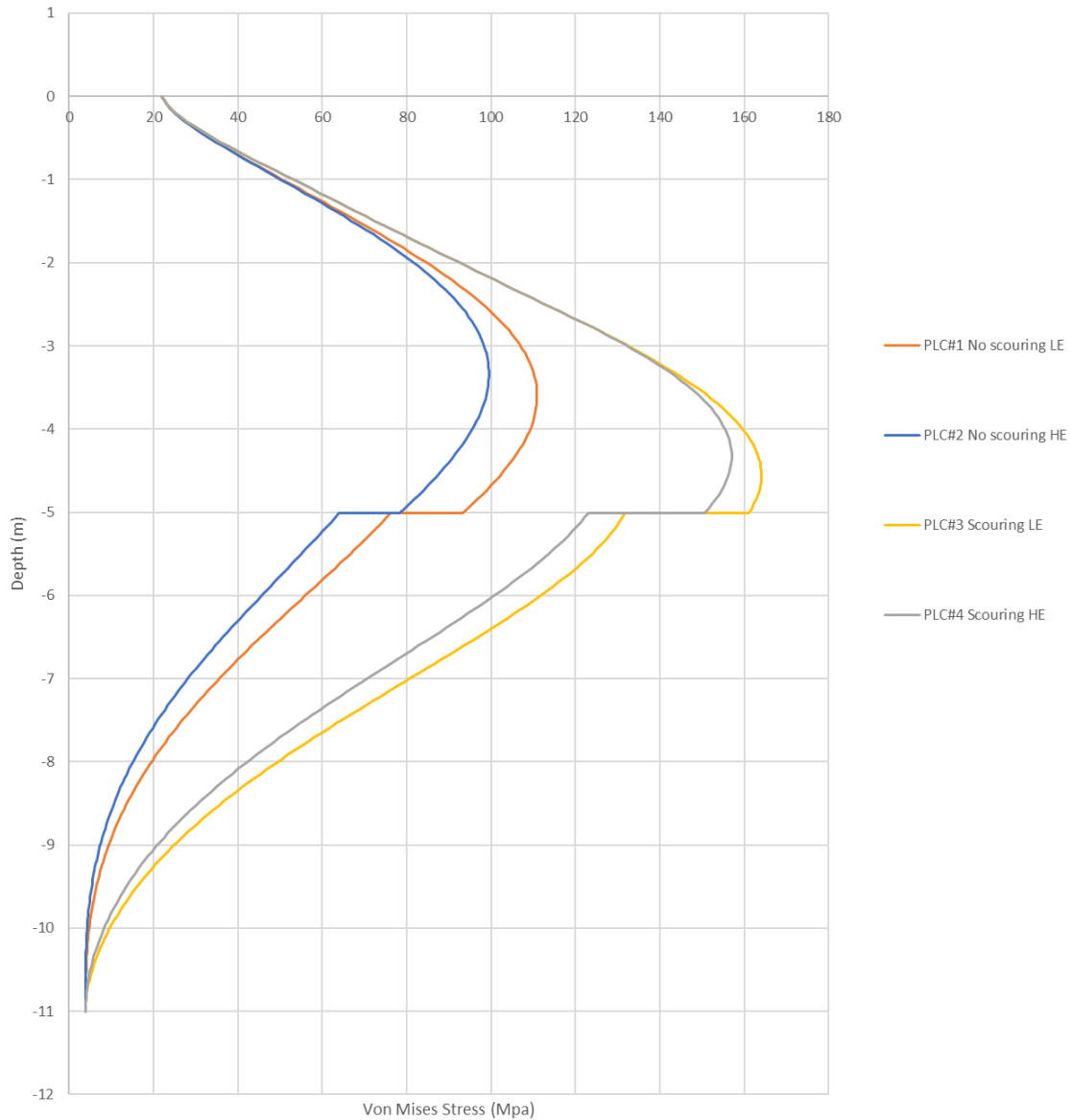


Figure 8: Von Mises stresses for load cases PLC#1-PLC#4

6.3.1. Buckling

A buckling check is performed according DNV-RP-C202 Sec 3.2-Sec 3.4.

The buckling check is performed by assuming the maximum normal stress and shear stress apply throughout a 13m pipe (embedded depth + stick-out). Soil around the pile is not considered to affect the buckling strength in this calculation.

The design equivalent Von Mises stress is well below the design buckling strength of the shell. Therefore buckling is not considered to be a problem.

Table 10: Buckling check results

Von Mises	164 Mpa
Elastic buckling strength from axial stress	2004 Mpa

Elastic buckling strength from bending stress	2091 Mpa
Elastic buckling strength from shear loading	328 Mpa
Reduced shell slenderness	0.51
Design buckling strength of a shell	298 Mpa

6.4. ALS load case

During an Accidental Limit State, the seaweed system has failed somewhere between the anchors and can therefore freely rotate around the anchors. In this scenario the anchor chain eventually may wrap around the pile.

As both load factors and loads are lower compared to the ULS, the soil resistances and pile capacities are not further evaluated. The ALS loads act unidirectional on the pad eye. A pad-eye load case of 337.9kN under 90 degrees and 47.9kN vertical is proposed. See table 2 for the ALS load case.

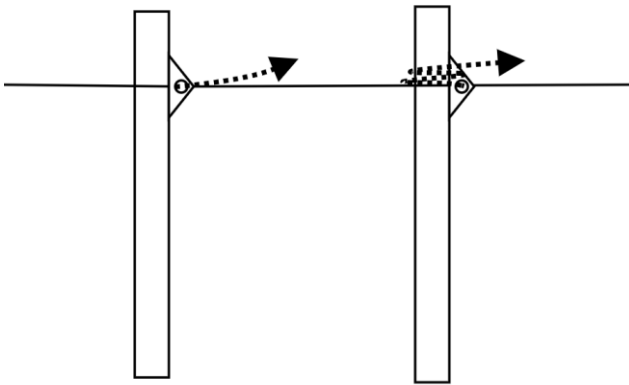


Figure 9: Situation during normal operation (left) and during ALS (right)

6.5. Pad-eye

6.5.1. Load cases

Loads have previously been determined and are shown in Table 5. Load cases with the largest lateral (PLC#1A) and axial (PLC#1B) are evaluated with FEM. As the load can be applied out-of-plane compared to the pad-eye orientation a horizontal misalignment is included in the load cases (including an installation tolerance of $\pm 2.5^\circ$)

A set of secondary load cases (PLC#2A & PLC#2B) with a higher horizontal misalignment angle are evaluated as well and function as a check (not a requirement!) and could potentially allow additional leeway for the installation tolerance. A final load case is extracted from the ALS specifications.

An overview of load cases that will be applied to the pad-eye is given in Table 11.

The pad-eye is at seabed, requiring to account for corrosion. All plate thicknesses are reduced by 4mm in the FEM model to account for corrosion.

Table 11: Pad-eye load cases

	Lateral load [kN]	Axial load [kN]	Horizontal out-of-plane angle compared to padeye [°]	Allowed stress Pad-eye [Mpa]	Allowed stress Pipe body [Mpa]
PLC#1A - Requirement	792 (688.8x1.15)	244 (212.5x1.15)	24.1	157	190

PLC#1B - Requirement	751 (653x1.15)	308 (268x1.15)	25.9	157	190
PLC#2A – Check	792	244	30	157	190
PLC#2B – Check	751	308	30	157	190
ALS	337.9	47.9	90	235	285

6.5.2. Model details

The FEM model is prepared in Fusion 360, which uses a NASTRAN solver. Linear material properties are used, as stresses stay below the yield point of the material.

The contact between the pin and hole is modelled as frictionless / sliding. A fixed support is added to the bottom of the pipe body.

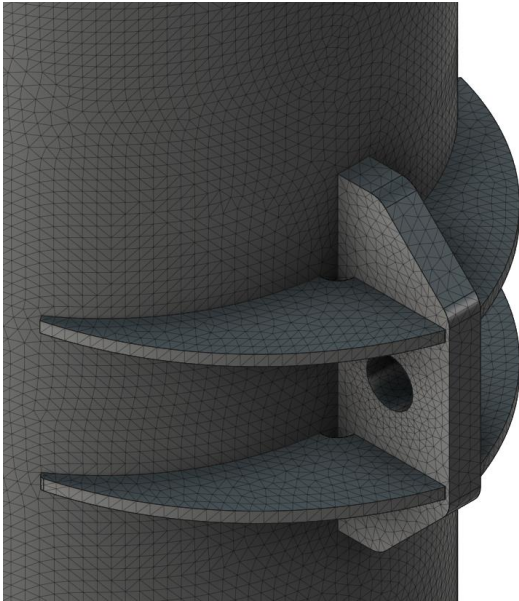


Figure 10: Mesh size

6.5.3. Results

The color scale in the results below is limited to 157 Mpa, the allowed stress for the pad-eye.

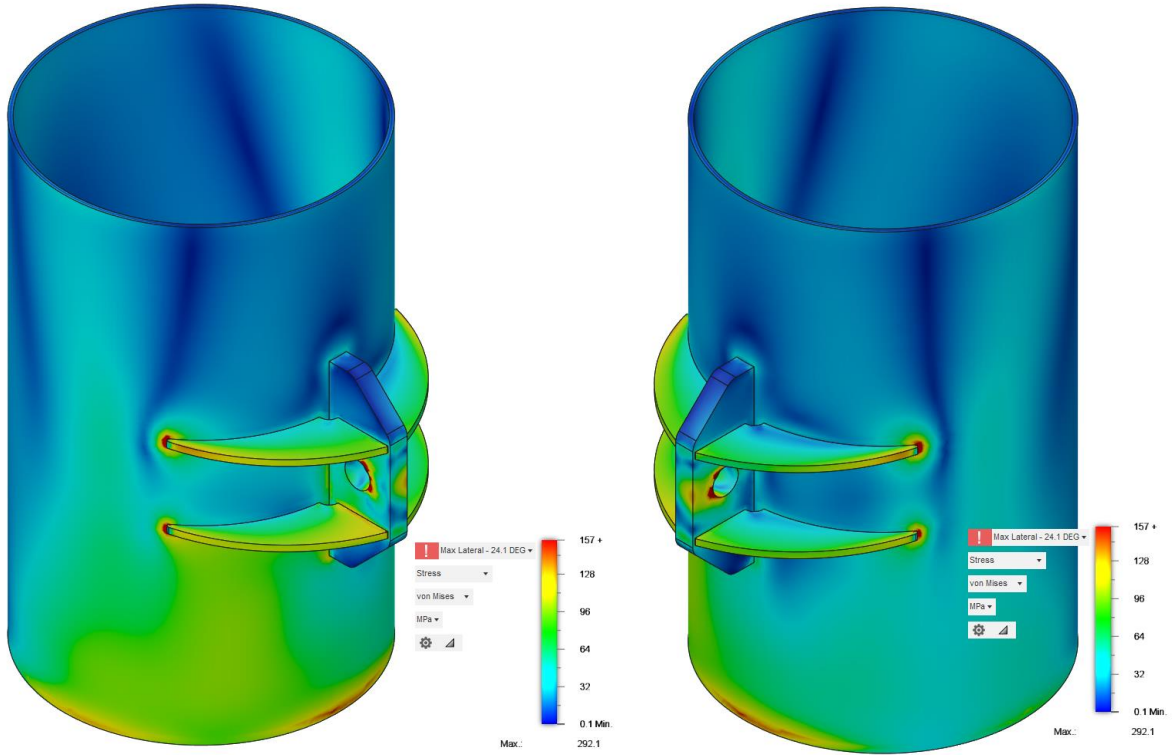


Figure 11: FEM results PLC#1A

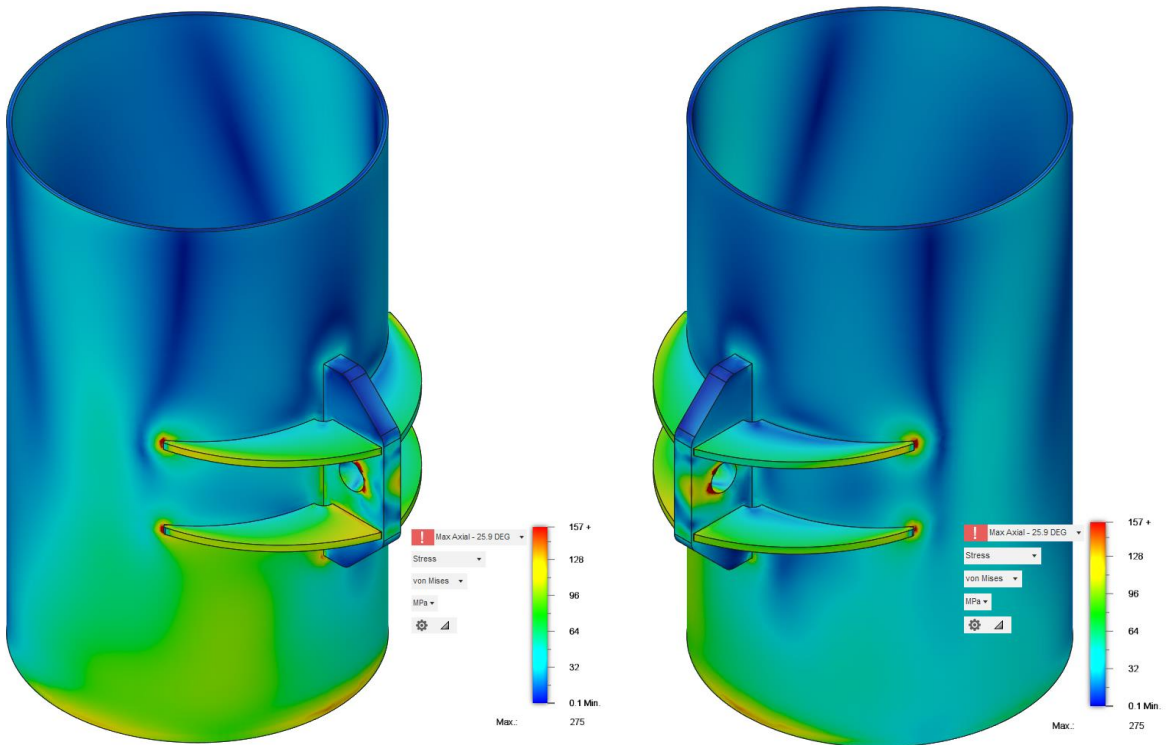


Figure 12: FEM results PLC#1B

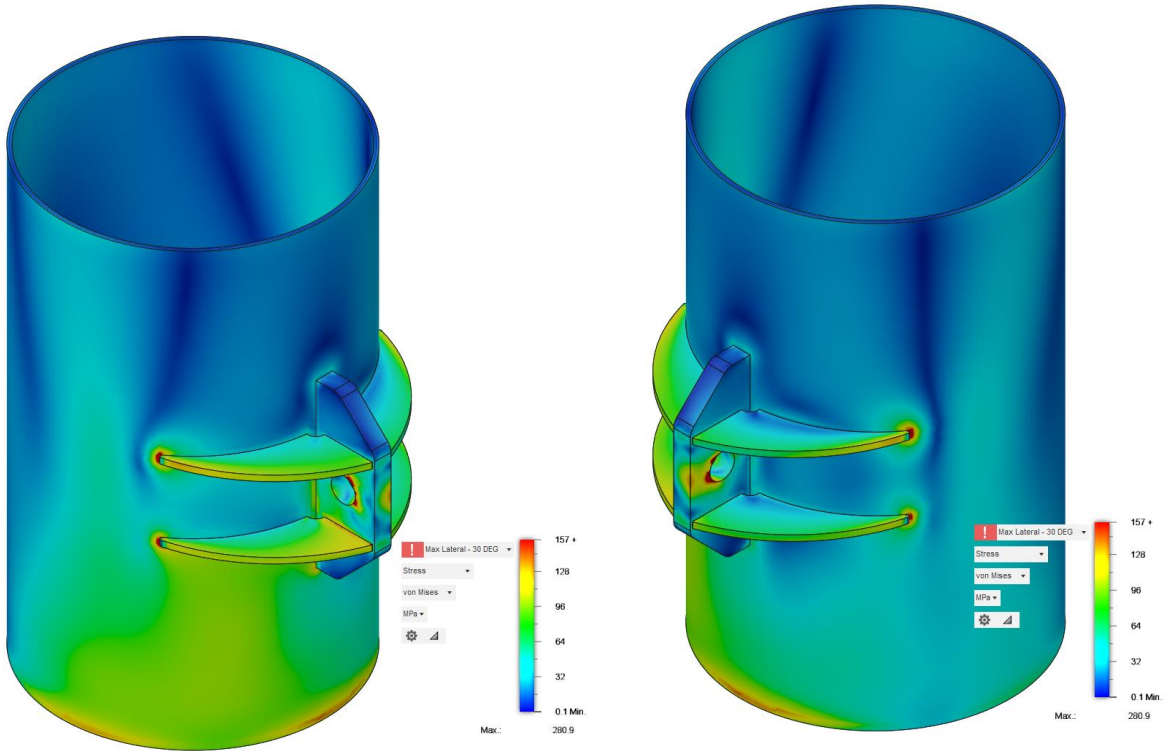


Figure 13: FEM results PLC#2A

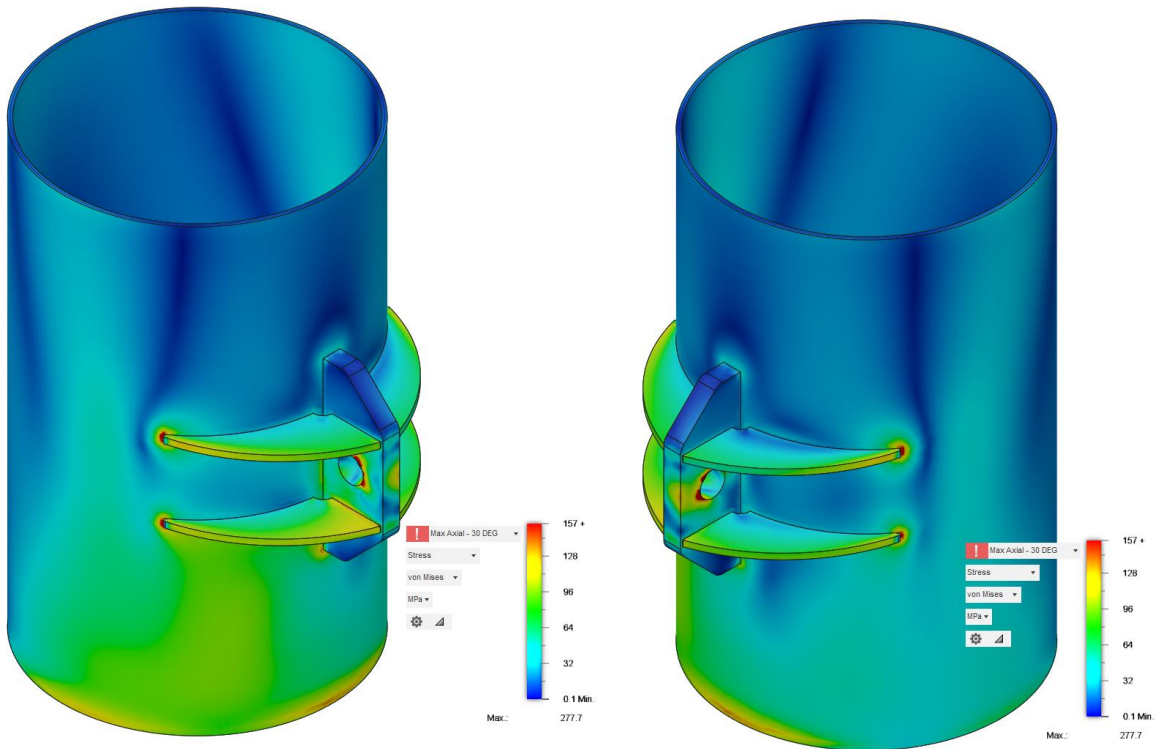


Figure 14: FEM results PLC#2B

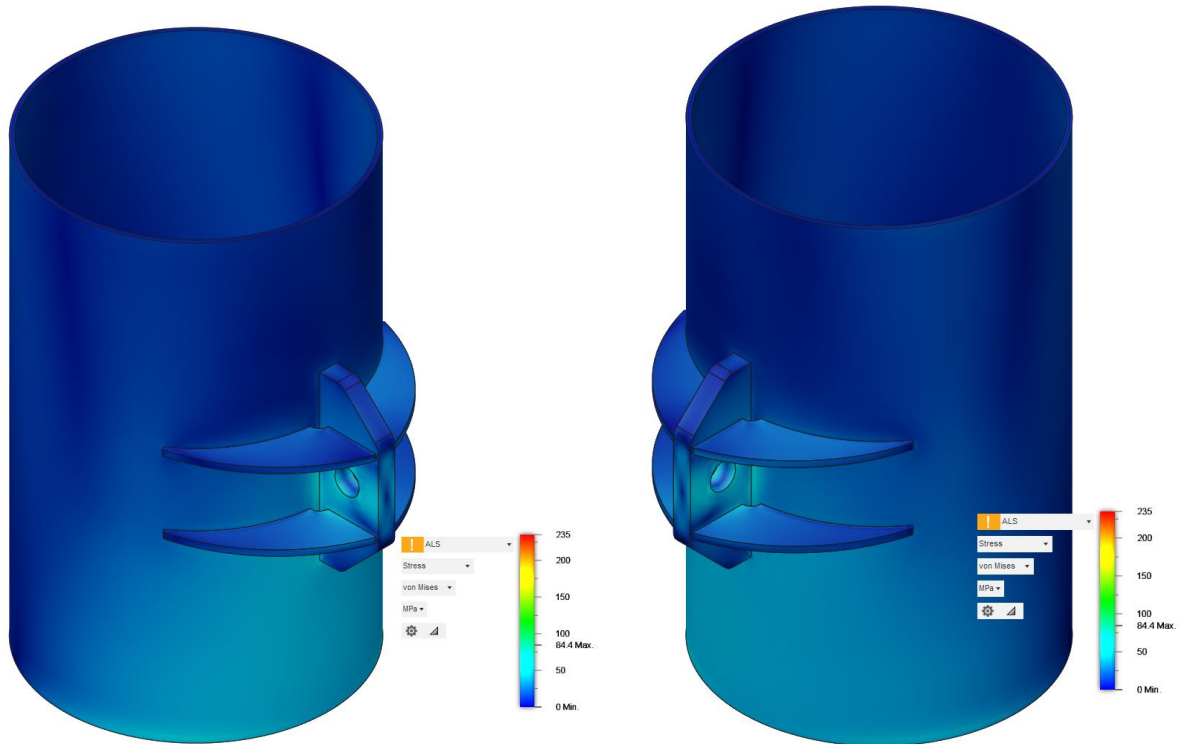


Figure 15: FEM results ALS

6.5.4. Interpretation of results

The results show that the stresses in the pad-eye are generally below the allowed stress. A few local hot spots are visible at the interface between the pin/shackle and pad-eye. A hand calculation is performed in the next section to confirm that these hot spots are allowed. Further on a hotspot (>157 Mpa) can be seen on the pipe body at the interface to the stiffener, the pipe body has a higher allowed stress (190 Mpa) and stresses in the pipe body are below 190 Mpa as can be seen in the figure below.

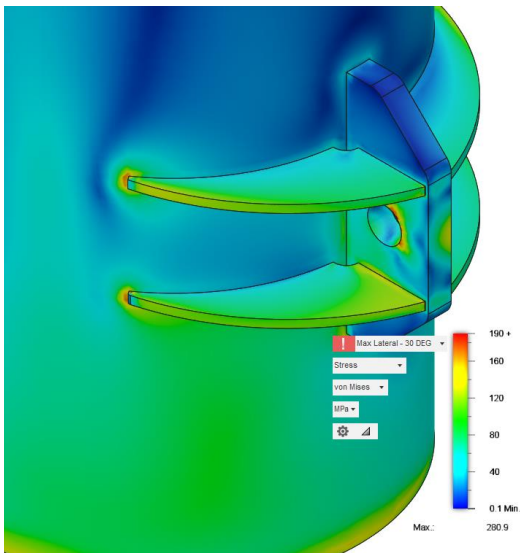


Figure 16: FEM Results PLC#2A – Color scale to 190 Mpa.

Additionally a weld calculation is performed in the next section to confirm the strength of the main weld on the pad-eye.

6.5.5. Hand calculation weld

For sizing of the weld the two load cases are applied to the main weld, neglecting the contribution of the stiffeners. A double sided PP20 weld is assumed; calculations are performed on a double sided PP18 weld including a corrosion allowance of 2mm (sub-seabed).

Table 12: Weld calculation according 2x PP18

	Lateral load [kN]	Axial load [kN]	Horizontal out-of-plane angle compared to padeye [°]	Comparison stress in weld* [Mpa]
PLC#1A - Requirement	792 (688.8x1.15)	244 (212.5x1.15)	24.1	151.2 Mpa
PLC#1B - Requirement	751 (653x1.15)	308 (268x1.15)	25.9	149.5 Mpa
PLC#2A – Check	792	244	30	160.8 Mpa
PLC#2B – Check	751	308	30	155.6 Mpa

*Calculated conservatively with NEN 2062 (art 5.4) and $\beta = 0.85$.

A minimum weld size of PP18 satisfies the requirements. The factor β is dependent on the steel grade and for S355 is 0.85.

According NEN 2062 the comparison stress must be below the yield point of the material. This is satisfied for all 4 load cases in Table 12. According the recommended design practice [4] a material factor (of 3) should be applied on the ultimate strength of the material, PLC#1A, PLC#1B and PLC#2B satisfy this criterion. PLC#2A (check, not a requirement) is slightly above the criterion (this load case with out-of-plane angle of 27.5° is within the criterion).

6.5.6. Hand calculation interface pin-hole

The interface between pin and hole shows peak stresses in the FEM model. To confirm that these peak stresses are allowed we calculate the average compressive contact stress in the pin hole:

$$\sigma_{\text{contact}} = \text{sqrt}(62700^2 + 473100^2) / (110 \cdot 80) = 54.2 \text{ Mpa} < \sigma_{\text{max,allowed}}$$

The stress is well below the criterion, thus the peak stresses in the FEM model are allowed.

6.6. Fatigue

The pipe body itself is not considered to be affected by fatigue. The main concern is the weld from the pad-eye to the pipe body. For this analysis the contribution of the stiffeners is neglected.

Fatigue load cases are given in the main structural report [1]. The highest fatigue load case (6.6m wave) has a maximum tension of 67 kN on the chain. Assuming this applies directly on the weld in the most unfavorable direction (normal with 30° high out-of-plane angle) we find a comparison weld stress of 12.8 Mpa.

If a wave period of 6 seconds is assumed, a total of $4.8 \cdot 10^6$ waves are expected during the design period of 10 years.

Whereas the S-N curve according DNV-RP-C203 for free corrosion with a fatigue category F3, $t=80\text{mm}$ and $\Delta\sigma=12.8 \text{ Mpa}$ has $23.3 \cdot 10^6$ allowable cycles. Thus even with this considerably conservative calculation, fatigue is not limiting.

7. Conclusion

All requirements are met by the pile design.

The installation tolerance can be increased to $\pm 5.9^\circ$ degrees compared to the $\pm 2.5^\circ$ set in [2] while the pile still satisfies all criteria. Further increase is likely possible with a more detailed (=less conservative) calculation approach for the pad-eye.

Load cases are extracted from [1] and are based on the MetOcean data from Borssele 3. It is assumed that the load cases for the pile are the same or lower when deployed at Hollandse Kust Zuid. Additional research is advised to confirm this.

Appendix A: Anchor loads from simulation results

For the Ultimate Limit State (ULS) 36 load cases have been simulated on the full farm scale [1]. From each simulation forces are extracted at the moment of highest lateral load and at the moment of highest axial load. These are shown in the table below.

For the Accidental Limit State (ALS) 10 load cases have been simulated, the ALS assumes the system is broken and thus only 1 anchor is considered.

The direction of the forces (F_{Lateral} and F_{Axial}) and angles (α_{vertical} and $\alpha_{\text{horizontal}}$) are indicated in Figure 17.

Table 13: From ULS simulation result extracted maximum loads on the anchor points at the mudline of the seaweed system. For each load case the loads (axial & lateral) and the angle (vertical = with seabed, horizontal = deflection) are shown for the moment where maximum lateral load and maximum axial load occurs. Forces are shown for the anchor with maximum load.

Load Case	F_{Lateral}	F_{Axial}	α_{vertical}	$\alpha_{\text{horizontal}}$	F_{Lateral}	F_{Axial}	α_{vertical}	$\alpha_{\text{horizontal}}$
	Maximum Lateral [kN]	Maximum Lateral [kN]	Maximum Lateral [deg]	Maximum Lateral [deg]	Maximum Axial [kN]	Maximum Axial [kN]	Maximum Axial [deg]	Maximum Axial [deg]
1	177.5	0.0	0.0	26.0	148.9	0.0	0.0	41.8
2	675.7	189.0	15.6	21.1	468.5	215.2	24.7	25.2
3	321.0	74.9	13.1	12.7	223.0	97.0	23.5	5.3
4	350.4	0.0	0.0	16.7	245.9	10.4	2.4	15.5
5	456.4	5.9	0.7	19.8	419.0	12.2	1.7	20.4
6	307.1	3.6	0.7	21.0	168.2	10.1	3.4	19.5
7	323.8	10.9	1.9	22.8	253.5	29.0	6.5	21.1
8	473.6	181.6	21.0	20.1	444.7	194.8	23.7	21.7
9	200.7	0.0	0.0	14.5	183.7	5.6	1.8	12.5
10	478.8	134.3	15.7	8.3	380.3	148.3	21.3	8.5
11	559.6	112.8	11.4	0.0	550.8	115.5	11.8	0.0
12	374.7	50.3	7.7	37.3	373.4	50.9	7.8	37.3
13	318.7	7.0	1.3	20.8	318.2	8.2	1.5	20.9
14	459.3	52.9	6.6	21.4	459.3	52.9	6.6	21.4
15	332.1	0.0	0.0	27.6	307.3	4.0	0.7	26.9
16	184.9	1.0	0.3	25.6	162.0	5.8	2.0	28.3
17	688.8	208.5	16.8	21.6	474.5	212.5	24.1	25.5
18	606.7	187.7	17.2	21.4	583.3	204.9	19.4	22.4
19	347.8	4.0	0.7	22.8	285.4	13.2	2.6	23.4
20	297.7	29.7	5.7	22.1	260.2	39.4	8.6	24.4
21	620.4	191.8	17.2	23.3	543.1	200.5	20.3	24.4
22	282.7	2.0	0.4	20.7	206.6	13.6	3.8	21.4
23	427.4	8.7	1.2	21.1	313.1	13.6	2.5	21.0
24	653.0	180.2	15.4	22.0	625.9	268.0	23.2	23.4
25	669.8	215.6	17.8	21.7	640.0	227.4	19.6	22.6
26	325.5	157.1	25.8	25.3	318.1	162.4	27.0	24.6
27	651.9	72.3	6.3	28.2	651.9	72.3	6.3	28.2
28	484.2	100.5	11.7	20.9	470.2	172.5	20.1	23.9
29	446.9	24.1	3.1	19.5	425.5	42.4	5.7	19.3

30	375.4	98.0	14.6	18.1	361.1	98.4	15.2	18.7
31	173.3	16.4	5.4	23.9	135.4	28.6	11.9	24.9
32	568.4	58.1	5.8	32.1	553.4	58.8	6.1	32.2
33	184.0	0.0	0.0	29.9	105.2	0.0	0.0	30.6
34	265.7	0.0	0.0	38.2	180.7	0.0	0.0	38.5
35	368.0	37.3	5.8	20.3	320.8	50.2	8.9	21.2
36	624.3	65.8	6.0	28.5	614.7	66.5	6.2	28.4
	Max Lateral 688.8					Max Axial 268.0		

Table 14: From ALS simulation result extracted maximum loads on the anchor point of the seaweed system. Note the angle of the mooring line is based on axial and lateral maximum occurring simultaneously and is not directly extracted from the simulations.

Load Case	F_{Lateral}	F_{Axial}	α_{vertical}	F_{Lateral}	F_{Axial}	α_{vertical}
	Maximum Lateral [kN]	Maximum Lateral [kN]	Maximum Lateral [deg]	Maximum Axial [kN]	Maximum Lateral [kN]	Maximum Lateral [deg]
201	289.6	0.0	0.0	279.2	8.4	0.0
202	337.2	13.0	1.2	308.7	15.9	0.7
203	142.8	0.0	0.0	125.1	0.0	0.3
204	212.7	0.0	1.0	208.9	3.4	1.2
205	276.9	3.1	0.0	272.1	3.5	0.0
206	148.7	0.0	0.0	97.7	0.0	0.0
207	217.5	0.0	0.0	178.7	1.9	0.4
208	83.3	0.0	0.0	64.5	0.0	0.0
209	337.9	17.2	0.3	287.8	47.9	0.1
210	220.4	0.3	0.0	199.7	2.7	0.0

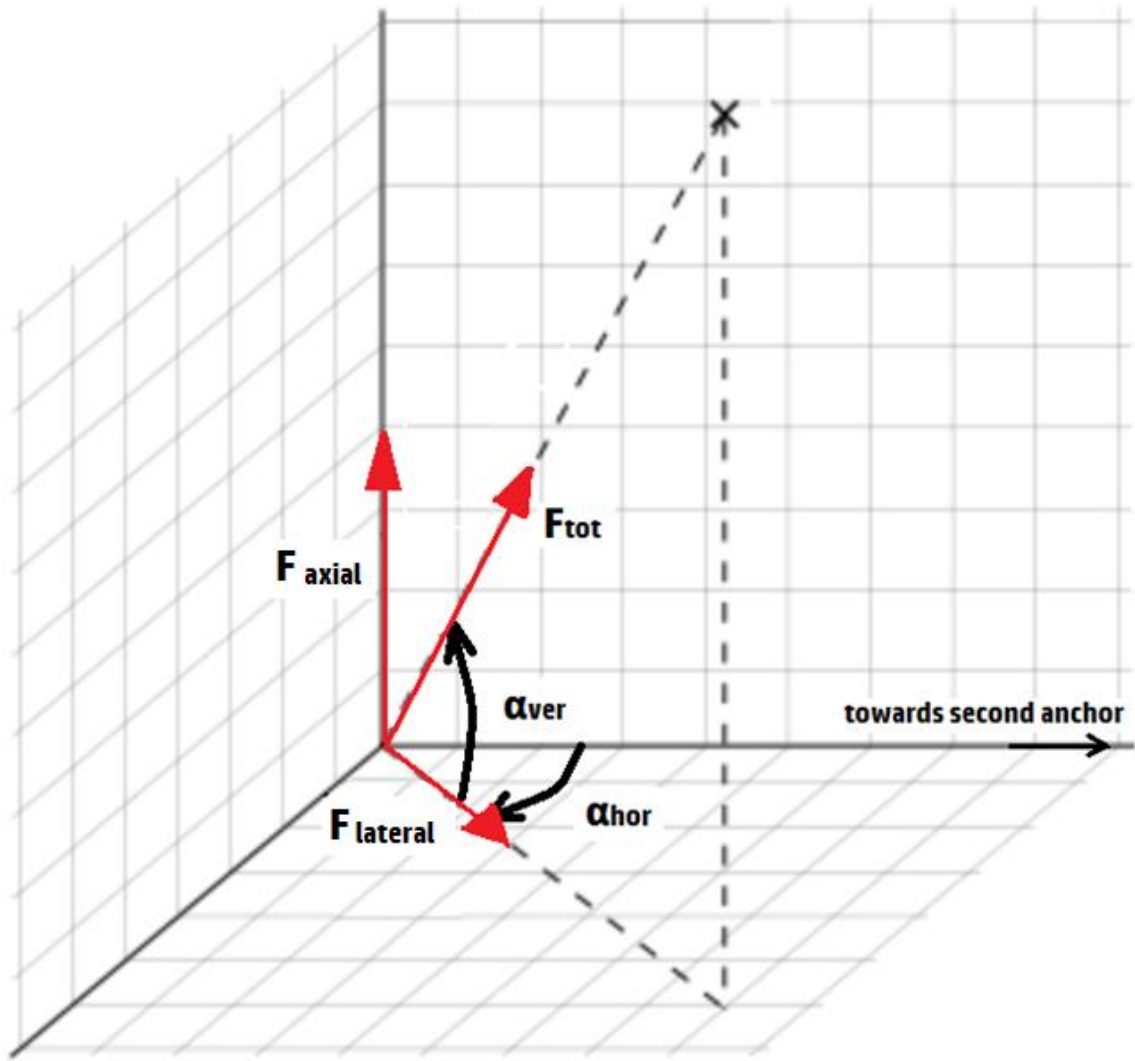


Figure 17: Visualisation of force direction and angles as indicated in the tables of this appendix.

Appendix B: Fit shackle

LTM \varnothing 58mm shackle and \varnothing 58mm chain end link.

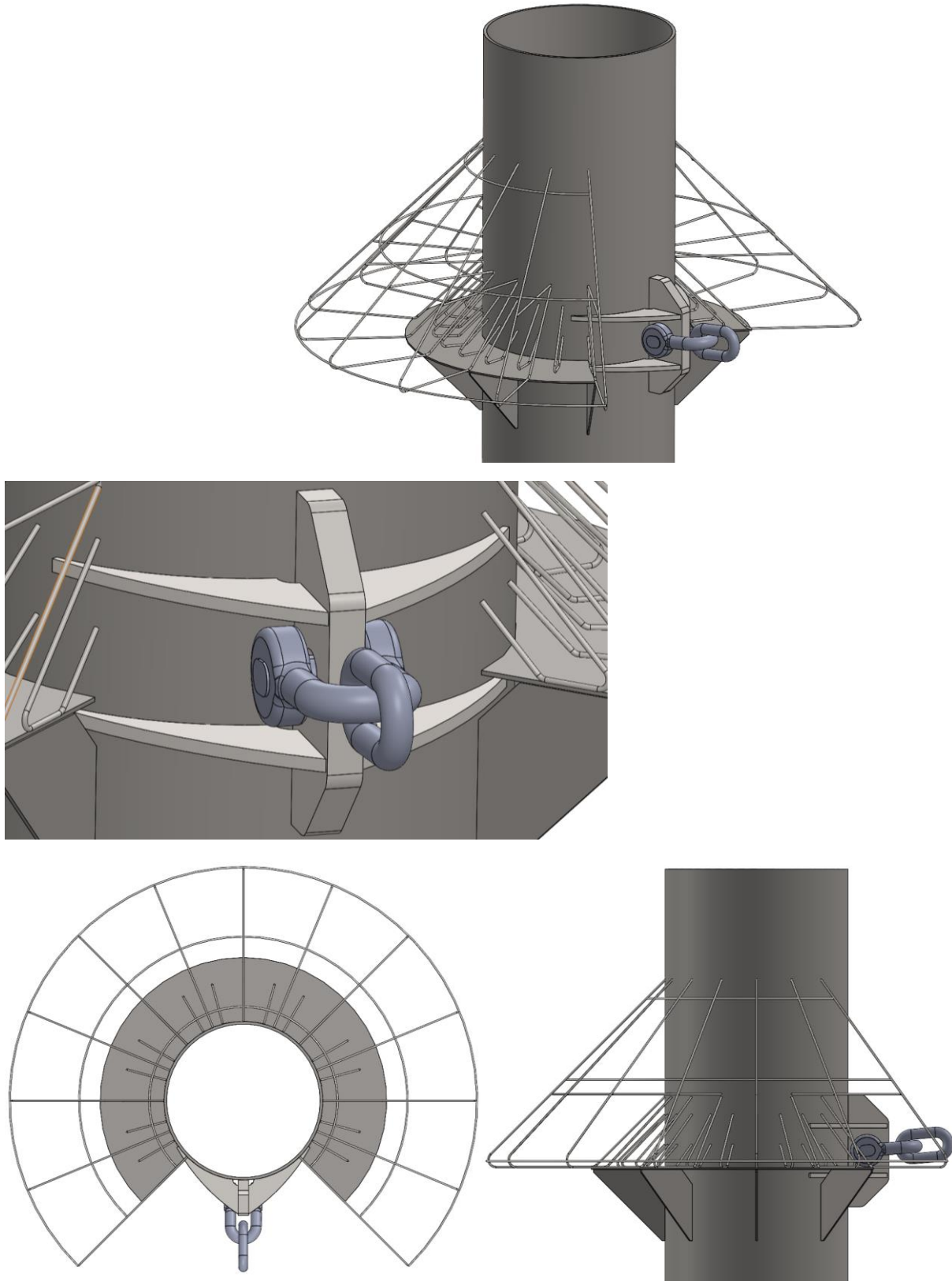
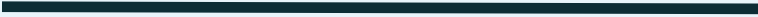
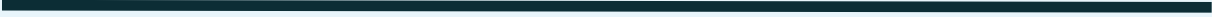


Figure 18: Screenshots pile including shackle and end link



www.aqitec.com



Aqitec Projects B.V.

All rights reserved

info@aqitec.com

Noordendijk 5

©2024

+31(0)641839404

3311RM Dordrecht

KvK 77153014

www.aqitec.com